CrossMark

Journal of Composites and Compounds

Application of polyoxometalate-based composites for sensor systems: A review

Hamid Khalilpour [a] , Parisa Shafiee [b]*, Amirhossein Darbandi [c], Mohammad Yusuf [d], Shirin Mahmoudi [e],

Zahra Moazzami Goudarzi [f], Sadegh Mirzamohammadi [g]

[a] *Department of Mining, Metallurgy and Materials Engineering, Université Laval, Québec, Canada*
[b] *Catalyst and Nano Material Research Laboratory (CNMRL), School of Chemical, Petroleum and Gas Engineering, Iran University of Science and Technology, Tehran, Iran*
[c] *Department of Mechanical Engineering, Payame Noor University, Tehran, Iran*
[d] *Department of Chemical Engineering, Universiti Teknologi PETRONAS, Bandar Seri Iskandar, 32610, Malaysia*
[e] *Semiconductor Department, Materials and Energy Research Center, Karaj, Iran*
[f] *Department of Chemical Engineering, Isfahan University of Technology, Isfahan, Iran*
[g] *Department of materials and Metallurgical Engineering, Technical and Vocational University (TVU), Tehran, Iran*

ABSTRACT

Composites based on polyoxometalates (POMs) have been increasingly attracted by many researchers due to their multitudinous architectures and excellent redox activities as well as outstanding proton and electron transport capacities. Lately, much research has been done on POMs composited with well-porous framework materials (including ZIFs, MOFs) or conducting polymers, carbon quantum dot (CQD), graphene, carbon structures (e.g. carbon nanotubes (CNTs)), and metal nanoparticles (NPs). The results exhibited improved stability and enhanced electrochemical performances. Hence, developing POMs and POM-based composite materials (PCMs) has long been a topic of interest for chemical researchers. Herein, the properties and applications of pristine POMs, doped POMs, and composite-based POMs are reviewed in detail. The various compositions of POMs with sensing application such as POMs-nanocarbon composites (POMs-graphene composites and POMs-carbon nanotube composites), POMs-conductive polymer composites, and POMs-metal composites are also investigated in this review. ©2021 JCC Research Group.

Peer review under responsibility of JCC Research Group

Table of contents

1. Introduction

Polyoxometalates (POMs) have an architecture made up of oxygen atoms and primary transition metals, such as Ta, Nb, W, V, and Mo in their maximum state of oxidation. Moreover, they significantly comprise

different heteroatoms including As, Si, P, and Ge. It would be possible to distinguish between the molecular oxides of POMs and most metal oxides. They include diverse metal atoms that contain about 368 metal atoms as nuclearities into an individual cluster molecule reaching nanoparticles. Berzelius firstly reported synthesizing POM in the 19th
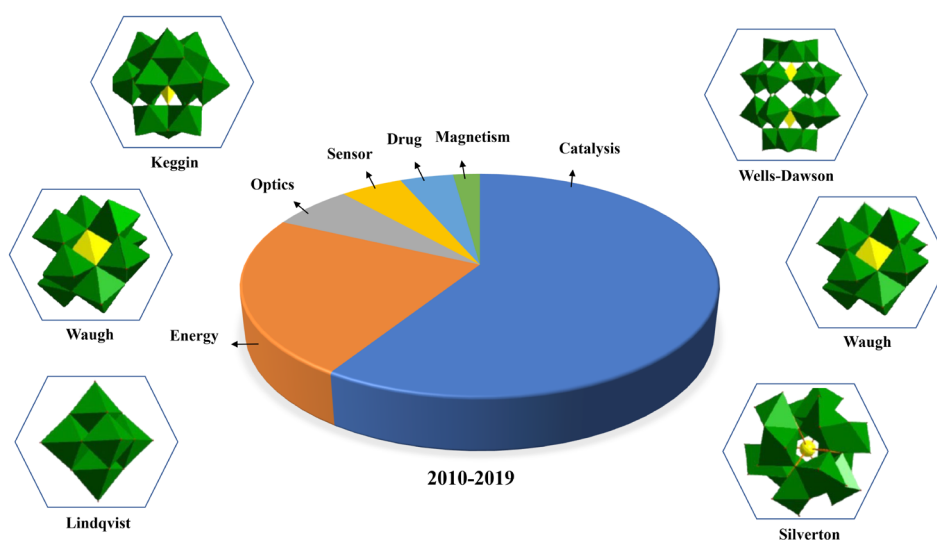
Fig. 1. Classical structure species of POMs and certain presented essential usages of POM-based structures in the recent decade.

century [1]. Besides, the oxoanions are occasionally assembled in a non-aqueous medium or a solid-state condition as in minerals. There are some properties to measure the stability of POMs in various solvents including aqueous/non-aqueous media lsuch as their ability to keep their structural properties and prevent declining or changing to other formations [2-5].

Many novel POM skeletons were uncovered, followed by the discovery of six classical systems such as Lindqvist, Dawson, Waugh, Keggin, Silverton, and Anderson (Fig. 1). Among the basic constructions of POMs, Dawson (X/M =2/18) and Keggin (X/M =1/12) are two main forms of POMs. Other complex structures are achieved by the accumulation of two or more Dawson or Keggin parts. The skeleton and composition of these forms of POMs depend on the employed methods and conditions. Some of the newly-generated POMs structures are ″sandwich″ type (a mix of the two lacunary entities of XW9 or X2W15 and H4XW15), ″crown″ or ″wheel″ type (a tetramer of the lacunary Dawson K12H2P2W12O48), and the ″banana″ type (two Keggin entities, XW-9M3O40 or XW9M2M'O40 are linked to XW6O16) [6, 7].

Numerous types of POM compositions with more intriguing and diversified structures have been shown by self-assembly of purely inorganic construction blocks and/or network bridging functions of organic ligands and metal ions due to the high activities of lacunary POM building blocks. For example, POM composite materials containing TMs, rare-earth ions (RE) replaced POMs, organic ligand, and heterometallic modified POMs, have been widely employed [1, 8, 9].

Because of their excellent electron and proton transportations and unstable redox behaviors, individual particle magnet activity and optical capabilities are already reported in POM-based composite materials (PCMs) [10-13]. In multi-electron reduction processes, POMs are good electron reservoirs. As a result, they can be used in the electrochemical field. Proton conductivity is another remarkable property of PCMs, allowing them to be used in modern perspectives, such as proton-exchange membrane fuel cells [10, 11, 14]. POMs, on the other hand, have been discovered to play a key part in the extraordinary development of PCMs having greater efficiency and stability. PCMs are also being used to create neoteric smart structures for applications such as optics [10, 11, 14], pharmaceuticals [15-17], energy-related applications [18-20], sensors [21-23], and green catalysis [24-26] (Fig. 1).

POMs are appealing for amperometric sensor applications because of their ability to sustain reversible multi-electron redox processes. They are particularly useful for detecting redox-active agricultural and industrial contaminants, including iodate, hydrogen peroxide, chlorate, nitrate, and bromate. POMs-based composites and nanocarbon structures, including carbon nanotubes (CNTs) and graphene, have gained much attention due to mixing the excellent chemical activity of POMs with the fascinating electronic properties of nanocarbon structures (a high surface area associated with electrical conductivity), which make them appropriate candidates for catalytic, energy-storing, energy conversion, electronics, and molecular sensor applications [27-30].

As sensing applications are among the most paramount research topics in technology these days, this paper reviews the fundamental properties of pristine POMs, doped POMs, and composite-based POMs in detail. Furthermore, and more importantly, the various compositions of POMs with sensing applications, such as POMs-nanocarbon composites (POMs-graphene composites and POMs-carbon nanotube composites), POMs-conductive polymer composites, and POMs-metal composites are investigated, a topic that has not been thoroughly investigated in other studies to this extent. This review is likely to pave the way for novel methods to modify POM-based composites in sensing applications.

2. Principal properties of POMs

Marignac [31] successfully discovered the synthesis way of 1:12 silico-tungstic acid in 1864. In the 20th century, Rosenheim first began the systematic analysis of POMs and the study of their characteristics. POMs are significantly able to adapt with and deliver a special number of electrons without any change or decomposition in their construction. Isopolyanions (IPAs) and heteropolyanions (HPAs) are components of POMs and are repeatedly created into aqueous media [32-34]. Besides, the oxoanions are occasionally assembled in a non-aqueous medium or a solid state as in minerals. There are some properties to measure the stability of POMs in various solvents, including aqueous/non-aqueous media such as their ability to keep their structural properties and prevent declining or changing to other formations. Among the basic constructions of POMs, Dawson (X/M =2/18) and Keggin (X/M =1/12) are two main forms of POMs. Other complex structures are achieved by the accumulation of two or diverse Dawson or Keggin parts [35-37].

That kind of POM based on a Keggin is formed by adjusting several metal atoms (M = Mo, Ta, W, Nb, V) around an individual heteroatom (X = Ge, As, Si, P). Pauling first proposed the Keggin structure in 1929 [1] and then it was approved by Keggin in 1933 [38]. In the Keggin
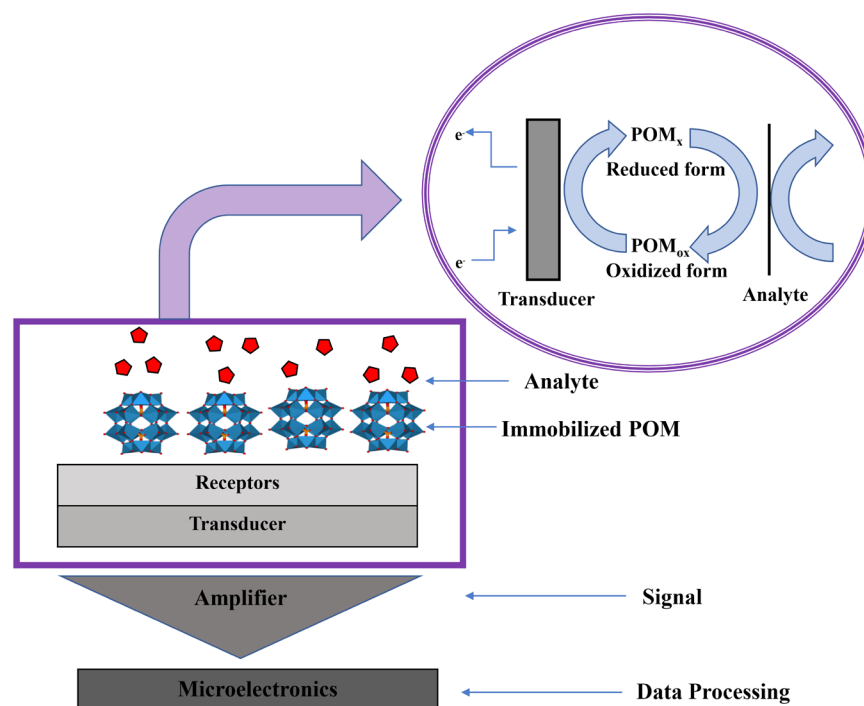
Fig. 2. Schematic design of the working process of a desirable POM-based electrochemical sensor.

structure, a tetrahedron is formed by the combination of the heteroatom X with four oxygen atoms and each metal atom with six oxygen atoms, makes an octahedral structure. The tri-metallic structures are linked to other networks and the typical place of M_3O_{13} is connected to the central heteroatom X [39].

Four oxygen atoms are bonded to the heteroatom X in the tetrahedron form of Keggin, and in the octahedron configuration, where every metal atom is bonded to six oxygen atoms. Because the Keggin type has three axes of symmetry, different rotations are also possible, resulting in more isomers. Although five types of Keggin structures are feasible theoretically, only three of them have been well identified, formed, and isolated. One or more metal centers would be lost by treating the Keggin structure of POMs with alkaline solvents under suitable laboratory settings including temperature, pH, and concentration [40, 41].

As a consequence, the lacunary POM species are achieved with the structure associated with the Keggin series. For instance, the decline of Keggin XM_{12} leads to both lacunary types of XM_9 and XM_{11}, having high stability and widely used in the following form. The produced lacunary types also possess multiple isomers. The lacunary Keggin structure of POMs can interact with transition metals (including NiII, MnII, ZnII, FeIII, and CoII) or other types of elements with close characteristics (MoV, WVI, VV) to complete the vacant positions and fabrication of the doped Keggin type of POMs [41, 42]. The reaction of transition metals (such as FeIII, NiII, MnII, CoII, and ZnII) or other close-aspect species (such as WVI, MoV, and VV) with lacunary Keggin POMs results in the formation of replaced Keggin POMs [1, 43].

Dawson POM dimer is constructed by combining two lacunary Keggin monomers $XW_9O_{34}^{z-}$, with X/M = 2/18. The first architectures of the Dawson structure were produced more than a century ago. For example, Souchay (1947) [44] proposed a dimer formation in Dawson as evidence of the proportion, X/M =2/18. Dawson POMs have two structures: (i) trimetallic groups (M_3O_{13}), which are shaped by the union of three octahedral WO_6 even though defined in the Keggin form, and (ii) the condensation of two octahedral with metal atoms in the centers and oxygen atoms in the vertices producing bimetallic groups (M_2O_{10}). Each group is connected to two $XW_9O_{34}z$ pieces and the heteroatom X to produce the Dawson structure. Other POMs are formed when lacunary types

from the Keggin or Dawson series react, and their composite and structure variations depend on the experimental attitudes [45, 46]. Sandwich form POMs, which lead to the composition of two lacunary entities, for example, XW_9 for Keggin or H_4XW_{15} and X_2W_{15} for Dawson dissymmetrical and symmetrical, respectively, through transition metal cations, are excellent candidates among the recently developed new structures (e.g., FeIII, MnII, CoII, NiII, ZnII). Weakley et al. [47, 48] identified the first synthesized sandwich POM in 1973. $K_{10}Co_4 (H_2O)_2(PW_9O_{34})_2$ is generated by two Keggin PW_9O_{34} moieties connected using four Co centers. Mbomekalle et al. [49] first announced the fabrication of a "banana" formation in the early 2000s, followed by Ritorto et al. [50]. This form resembles a sandwiched POM to make a banana formation of POM, with two Keggin structures, $XW_9M_2M_0O_{40}$ or $XW_9M_3O_{40}$ (M and M_0 are various metal species) being bound to an XW_6O_{16} component. Other POM formations with excellent multi-dimensions have been fabricated to extend their functionalities. Some POMs are synthesized by varying the bond lengths, such as $H_6B_3W_{39}O_{13215}$ and $H_6B_2W_{26}O_{90}$, which are made of trimers or dimers of $H_3BW_{13}O468$ [45, 46]. Lastly, more complicated designs have been created using self-assembly processes combining organic ligands and polyoxo-anions [45, 51].

POMs have a wide range of content, structure, size, and charge, resulting in a large number of characteristics. In an aqueous solvent, for example, the majority of POMs exhibit solubility trends and act as strong acids [46]. The Hammett acidity constants (Ho) of the dense media of $H_3PW_{12}O_{40}$ and $4SiW_{12}O_{40}$ using water solutions containing 94.5% acetic acid and 40% aqueous dioxane were determined by Khozhevnikov et al. [52]. The acidity of $H_3PW_{12}O_{40}$ is higher than that of H_2SO_4 or $HClO_4$, as can be shown. Mineral acids, such as H_2SO_4 and H_3PO_4 can be replaced by POMs in homogeneous catalytic processes. Inorganic media, POMs, for example, show medium-dependent insolubility [53].

POMs can be considerably altered when mixed with organic moieties including ionic liquids or quaternary ammonium salts [54]. Certain POMs exhibit luminous properties; others, which include ferromagnetic transition metal atoms with free electrons, display anomalous magnetic characteristics and are being studied as nano-computer storage systems. Certain possible green outlooks of POMs have been studied including a nonchlorine-based, way of decontaminating water, and the wood pulp

Table 1.

Some characteristics of POM composite-based sensor systems

Author/Ref.	Composite	Target Substance	Linear range (µM)	Detection limit (µM)
Qian et al. [74]	POM@mrGO	NADH	5.0×10^{-9} M-5.0×10^{-4} M	0.4 nM
Yokus et al. [75]	POM-rGO/GCE	l-tyrosine (l-Tyr) and l-tryptophan (l-Trp)	1.0×10^{-11}–1.0×10^{-9} M	2.0×10^{-12} M
Yola, et al. [75]	rGO/POM	triclosan	0.5–50.0 nM	0.15 nM
Li et al. [76]	MWNTs/PMo12	bromate	5 µM-15 mM	0.5 µM
Ertan et al. [77]	PtNPs/POM/MWCNs/GCE	simazine	1.0×10^{-10} - 5.0×10^{-9} M	2.0×10^{-11} M
Haghighi et al. [78]	GCE/MWCNTs/[C8Py][PF6]-PMo12	IO_3^-	2×10^{-5}-2×10^{-3} M	15 µM
		H_2O_2	2×10^{-5} -8×10^{-3} M	12 µM
Anwar et al. [79]	Cu^{2+}/ POM- 2 mM	H_2O_2	up to 2 mM	0.3 µM
	Fe^{3+}/POM-doped polypyrrole			0.6 µM
Ayranci et al. [80]	POM/PAAC	glucose	0.1-10 mM	0.099 mM
Babakhanian et al. [81]	PPy–α-POM–AuNPs	folic acid	-	12 nM
Wang et al. [82]	Pd/POMs/NHCSs	acetaminophen	0.63 µM -0.083 mM	3 nM
Karimi-Maleh et al. [83]	PtNPs/POM/2D-hBN	N hydroxy succinimide	0.1-300 µM	60 nM
Zhang et al. [64]	$Ru(bpy)_3Cl_2 \cdot 6H_2O$ $H_7P_2Mo_{17}V_1O_{62}$ ($P_2Mo_{17}V$) ($Ru(bpy)_3$) /chitosan-palladium (Cs-Pd),	ascorbic acid	0.125–118 µM	0.1 µM
Zhou et al. [65]	$(P_2W_{16}V_2$-AuPd/PEI$)_8$	dopamine	2.1×10^{-6}-2.06×10^{-3} M	8.3×10^{-7} M
		ascorbic acid	1.2×10^{-6}-1.61×10^{-3} M	4.3×10^{-7} M

bleaching method. Numerous medicinal and biological characteristics of POM structures have been studied such as anti-bacterial, anti-viral, and anti-tumoral aspects [55, 56]. Fluorescent microspheres produced from Lindqvist POM covalently linked to pyrene groups, for example, have been used to detect foodborne illnesses [57, 58].

POMs, including inorganic molybdenum and/or tungsten with rare earth (RE) cores, were also demonstrated to be good illuminating probes. Cryogenic optic thermal probes made of polyoxomolybdate basic elements containing TbIII and EuIII ions, for example, have been explored. Moreover, the luminescence properties of RE-combining POMs are significantly delicate to the chemical media [59, 60].

Brown and blue POMs are formed when POMs are decreased. POMs in their oxidized form may adapt to and provide a specified quantity of electrons with no modification or disintegration in their construction. Except in rare circumstances where production is curtailed without adequate stability in the mixture, re-oxidation of reduction in POMs formation reforms oxidation structures. POMs-based redox systems are electrochemically quick in general. As a result, decreased POM formations can participate in numerous electrocatalytic cycles [61, 62].

To capitalize on these redox characteristics, POMs are selectively deposited on substances for heterogeneous electrocatalysis. Many researchers, who worked in the field of immobilized electrochemistry POM structures on solid surfaces, observed that the physicochemical features of POMs were frequently conserved after immobilization. Analytical devices, including a POM-based sensor that includes a POM rendered immobile on a solid surface are known as the transducer [61, 63]. Unless the POM's characteristics and structure after immobilization are preserved, this will catalyze and identify the analyte. The chemical process method caused by the distinction between both the analyte and then the immobilized POM would be converted to an electric signal, that will be amplified and transformed into a demonstration via a signal processing instrument (Fig. 2). The detection limit and stability, response time, sensitivity, linear range, and selectivity are all important properties of a POM-based sensor, the same as other sensors [64].

3. Insertion of dopant ions in POMs

Chemical modification of the POM formation, such as the incorporation of redox-active metal centers, can fine-tune the exact electrochemical characteristics including the number of electrons stored and redox potentials [65, 66]. Shi et al. [67] created polyoxometalates (POMs) and TiO_2 nanostructured materials by combining various POMs, including K_5 $[PW_{11}TiO_{40}]$ and titanium-substituted POMs K_7 $[PW_{10}Ti_2O_{40}]$ with TiO_2 nanoparticles to modify the crystalline structure of TiO_2 nanoparticles. In addition, the photoconductivity of TiO_2/POM nanocomposites is proportional to the difference in conduction bands between TiO_2 and POMs. Furthermore, TiO_2/$PW_{11}Ti$ demonstrated excellent acetone gas sensing capabilities. These findings show that TiO_2/POM nanocomposites have excellent photoelectric characteristics as compared to pure TiO_2 nanoparticles, which is due to the interface modification with various POMs. Using cationic poly (diallyl dimethylammonium chloride) functionalized reduced polyoxometalates clusters $K_8P_2W_{16}V_2O_6$ combined with anionic Au nanoparticles ($P_2W_{16}V_2$-Au) and graphene oxide. Bai et al. [68] developed an accurate electrochemical biosensor for UA detection (PDDA-rGO). The effective combination of PDDA-rGO and $P_2W_{16}V_2$-Au offers several advantages in electrochemical detection, including more sensing sites, unimpeded diffusion pathways, and faster electric charge transfer. Under optimal circumstances, the amperometric i-t sensitivity of a modified PEI/[$P_2W_{16}V_2$-Au/PDDA-rGO] electrode was used to add different densities of UA to a swirling 0.2 M PBS (pH = 7.0) for 1700 s at 50 s former at a potential range of +0.43V, resulting in good analytical results for UA. The electrode has a consistent and well-defined amperometric response to the supplied UA, with the responsiveness of lefewerhan equal to 3 seconds. The calibration plot demonstrates a satisfactory linear correlation in the range of 2.5×10^{-7} - 1.025×10^{-4} M, with R_2 = 0.9912. I = -0.01406 + 0.24092 × CUA, which denotes the linear regression model. The limit of detection (LOD) is 1.4
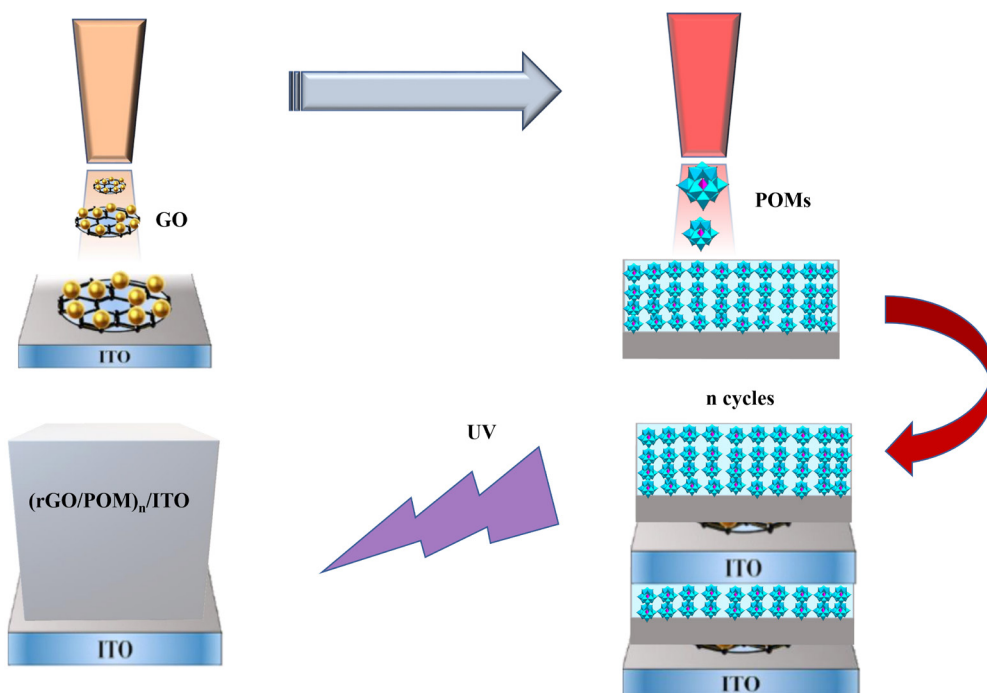
$\times 10^7$ M, and the responses are 0.24 A M1 based on a signal-to-noise ratio of 3 (S/N = 3).

Shen et al. [69] produced L-cysteine-doped tungstosilicate (Lcys-SiW$_{12}$) microtubes by altering them slightly. The ammonia gas sensitivity of synthesized Lcys-SiW$_{12}$ microtubes is demonstrated by the unique color change of microtubes from a purple color after being exposed to ammonia gas turning to a dark blue color throughout the skin. The adsorbed ammonium molecules may raise the basicity of the Lcys-SiW$_{12}$ microtubes, hence enhancing the redox process between L-cysteine and polyoxometalate, as a possible method for the coloration. The proton capture agent initiates a pH-dependent solid-solid redox process. Alkaline gas chemical sensors have been developed using Lays-SiW12 microtubes.

Sensitive analytical procedure enhancement, which is significant for a healthy lifestyle, was reported by Medetalibeyolu et al. [70]. The electrochemical behavior of electrodes was studied using hexagonal boron nitride (2D-hBN) nanosheets, molecularly/polyoxometalate (POM), and gold nanoparticles (AuNPs). Cyclic voltammetry (CV), differential pulse voltammetry (DPV), electrochemical impedance spectroscopy (EIS), and imprinted polymer (MIP) were also employed in their work. The DIA imprinted electrode had a highly sensitive response to DIA as-fabricated and presented a wide linear range. In addition, the LOD was 3.0×10^{-12} M. The modified detector was successful in detecting DIA in fruit juices [68].

Triacetone triperoxide (TATP), a homemade explosive, is simple to make and sensitive to the selection, but difficult for detection directly. Vapor sensing using arrays made up of only a few distinct sensor materials can differentiate TATP; however, manufacturing a stable sensor has always been difficult since each sensor may experience a device malfunction [71, 72]. To identify TATP from other explosives, a sensor array built on a single photonic TiO$_2$/PW$_{11}$ sensor was created initially, with the excitation wavelength being controlled. Situ doping of Na$_3$PW$_{12}$O$_{40}$ on TiO$_2$ resulted in the production of a Keggin type of PW$_{11}$, which increased the sensor film detection sensitivity and response time, and facilitated photo-induced electron-hole separation, according to Lu et al. [72]. The TiO$_2$/PW$_{11}$ sensor film has TATP sensitivity at 81, 37, and 42% under 365, 550, and 450 nm illumination, respectively. The TiO$_2$/PW$_{11}$ sensor has TATP selectivity and can measure concentrations of less than 50 ppb. The amount of bending also demonstrates the stability and flexibility of the flexible sensor film. Moreover, ambient air with a relative humidity of less than 60% cannot influence the sensing response [73].

4. POM-based composites for sensor systems

Over the last decade, several PCM architectures have been developed under various preparation conditions. According to their various hybrid structures, PCMs are divided into three groups in this review: (1) POM-based conductive polymer composites, (2) POM-based nanocarbon composites, and (3) POM-based metal composites, which are all examples of POM-based composites. The characteristics of various POM composite-based sensors are indicated in Table1.

4.1. POM-nanocarbon composites

The enhancement of developed composition materials based on nanostructured carbons and POMs has garnered a lot of attention because they combine the incredible electronic properties of nanocarbon with the desirable chemical reactivity of POMs. The ability of POMs to initiate changeable multi-electron redox processes makes them appealing for amperometric sensor applications. Because of their capacity to trigger variable multi-electron redox reactions, POMs are intriguing for amperometric sensor usages. To achieve low selectivity, POMs must be immobilized or anchored on conductive substrates to maximize amperometric response while preserving molecular distribution. As a result, graphene and CNTs make excellent sensor substrates [25, 67, 84].

4.1.1. POM-graphene composites

Carbon compounds enhance the conductive surface area. Because of the strong electrical interactions among carbon materials and POMs, electrochemical features of carbon materials and POM compositions have been developed significantly [85-87]. Ji et al. [88] have recently proposed a highly advanced technique for nanocarbon layered electrodes/POM that could be used for automated and large-scale produc-
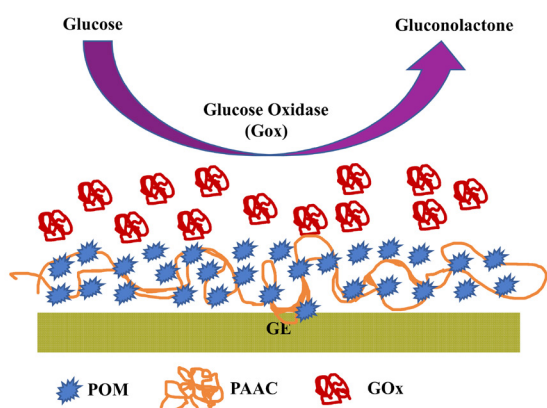
Fig. 4. Schematic design of a sensor platform contained metal/organic hybrid composite film based on POM/PAAC.

Fig. 5. The schematic of the synthesis of PPy–α-POM–AuNPs film; the Au electrode is shown schematically.

tion. The team used inkjet printing and a combination of layer-by-layer (LbL) processes for assembling the layered PW12/rGO composites (Fig. 3). LbL growth of a thin-film composition was linear, regular, and uniform. A POM-driven photo-reduction transformed GO to rGO under ultraviolet light, and the components were employed as high-response dopamine sensor devices.

Zhang et al. [89] used a layer-by-layer inkjet printing technique to make a multilayer film out of polyoxometalates such as $H_3PW_{12}O_{40}$ (PTA) and graphene oxide (GO) nanosheets. The composition of PTA/rGO film has an excellent electrocatalytic activity for the oxidized dopamine DA, according to cyclic voltammograms measurements. The oxidation peak current (Ipa), which can be used in electrochemical biosensors, increases gradually as the dopamine concentration rises.

The composition of polyoxometalate (POM) versatility coated reduced GO (POM@mrGO)/magnetic Fe_3O_4 as an embolization composite for the electrochemiluminescence (ECL) agent by bpy^{32+} was investigated by Qian et al. [90]. When compared to $Ru(bpy)^{32+}$ /Nafion@mrGO, which is increasing due to POMs high electro-catalytic interaction towards NADH oxidation, the efficient modification of POM@mrGO/Ru(bpy)$^{32+}$ hybrid easily implicated a magnetic electrode for about the equal density of nicotinamide adenine dinucleotide (NADH), which also resulted in a 10-fold increase in ECL intensity. The stable and ultrasensitive ECL monitoring of NADH at concentrations as low as 0.1 nM was made possible by this sort of finding. The manufactured biosensor has an extraordinarily decreased LOD of 0.4 nM and outstanding efficiency, with a linear curve range extending from 5.0 10^{-9} M to 5.0 10^{-4} M. This sensing technique may be defined as a biocompatible and novel substrate for dehydrogenase-based ECL biosensors since it combines facile sensor production with enzymatic selectivity. This research demonstrates a simple method for immobilizing ECL types within the versatile POM@mrGO support matrix and encourages the enhancement of magneto-controlled ECL biosensing for use in bioanalytical and analytical fields [32].

Yukos et al. [91] developed a polyoxometalate ($H_3PW_{12}O_{40}$, POM) and reduced graphene oxide (rGO) to change glassy carbon electrode (GCE) voltammetric sensor for concurrent determination of l-tryptophan (l-Trp) with l-tyrosine (l-Tyr). One of the developed methods was also used to successfully determine l-Tyr and l-Trp in spiked serum samples, with the LOD of 2.0×10^{-12} M and the linearity range of 1.0×10^{-11} - 1.0×10^{-9} M. Because of its widespread use in medical equipment, personal care products, and household cleaning products, triclosan (TCS) poses a significant risk to the environment and human health due to its toxic effects on aquatic organisms and leakage into groundwater supplies, surface water, and sediments.
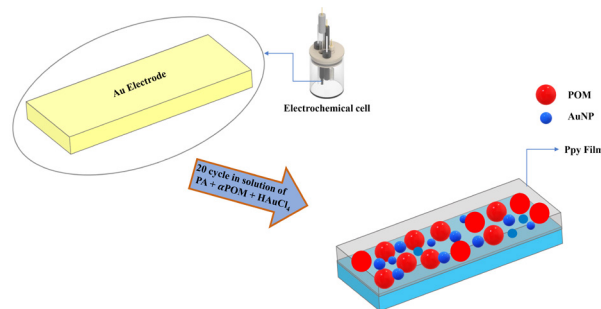
Yola, et al. [76] invented a molecular-imprinted reduced GO/gold nanomaterials electrochemical sensor decorating polyoxometalate ($H_3P-W_{12}O_{40}$). The functionalization of rGO using POM to produce a photocatalyst (rGO/POM) in an aqueous solution for detecting traces of TCS within wastewater via electrostatic interaction between rGO and POM nanosheets. Without using any reducing agent, gold nanoparticles (AuNPs) were deposited on the rGO/POM, and the synthesized nanomaterial (AuNPs/POM/rGO) was used for the modification of a glass carbon (GC) electrode (AuNPs/POM/rGO/GC) under infrared light. TCS-imprinted film was created on AuNPs/POM/rGO/GC using TCS and phenol polymerization and characterized using cyclic voltammetry (CV) and electrochemical impedance spectroscopy (EIS). TCS limit and linear detection range of the sensor were found to be 0.15 nM and 0.5 – 50.0 nM, respectively. When compared to other complicated methods, the molecularly imprinted sensor performed well on lake water samples and wastewater.

4.1.2. POM-carbon nanotube composites

Iodate and bromate are suspected carcinogens that are formed in drinking water as a result of ozone treatment. As a result, in situ detection is a hot topic in the industry. Li et al. [76] solved the problem by developing an MWNTs/PMO_{12} composite film based on an amperometric bromate sensor. The device feature has a 5-15 mM linear range, reaction times of less than 2 s, a sensitivity of 760.9 μA mM^{-1}.cm^{-2}, and a LOD of 0.5 M.

Based on this research, Qu et al. [77] conceived and developed MWNTs methyl silicone oil and a set of electrodes made of carbon nanotube paste (CNTP). Direct and indirect methods were used to assemble Keggin and Dawson types of POM anions on the CNTP electrode surface. The Dawson-anion of P_2MO_{18} structure proved to be a promising device, demonstrating effective bromate and iodate electrocatalytic reduction. A follow-up study used the LbL approach to create multilayered films of (P_2Mo_{18}/PDDA)$_n$ on CNTP electrodes, and comparative studies demonstrated that the LbL-assembled composites had higher electro-catalytic activity than the direct electrostatically generated composites.

Gue et al. [78] devised a chemically modified electrode with the distribution of CNTs in cationic chitosan films and applied it for electrostatically-immobilized Dawson anions of the P_2W_{18} structure. Electrochemical investigations showed that the P_2W_{18}/CNT/chitosan electrode had strong electrocatalytic activity, a fast response to reduce peroxodisulfate iodate, anions in acidic aqueous media. It was also stated that the sensor performed in acidic solutions, enhancing its application in different industries.
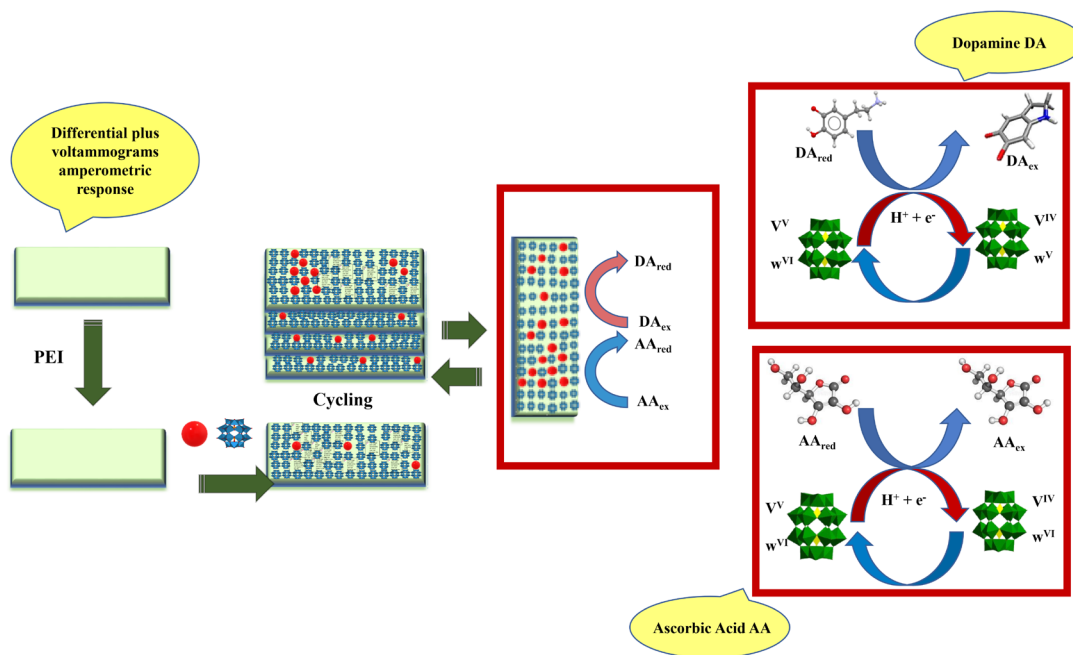
Fig. 6. The schematic design of the layer-by-layer self-assembly method.

To assess simazine (SIM), novel molecular imprinting voltammetric sensors are built on a glassy carbon electrode (GCE) altered with platinum nanoparticles (PtNPs) included in polyoxometalate ($H_3PW_{12}O_{40}$, POM) functionalized multi-walled carbon nanotubes (MWCNs) sheets as reported by Ertan et al. [79]. SIM imprinted GCE was synthesized by electro-polymerizing 100 mM pyrrole as the unit in 0.1 M acetate buffer (pH 4.0) with 25 mM SIM LOD. The linearity ranges of the developed method were determined to be 2.0×10^{-11} M and 1.0×10^{-10} - 5.0×10^{-9} M, respectively. Water samples were also tested using the voltammetric sensor.

Sahraoui et al. [92] successfully designed a Keggin-type metatungstate hybrid POMs ((APy) $6[H_2W_{12}O_{40}]$)/carboxylic acid-synthesized SWCNT-based amperometric sensor for hydrogen peroxide sensing. In the existence of SWCNTs, the sensitivity of hydrogen peroxide detection enhanced by a factor of 38.5, demonstrating their strong effect on peroxidase-like mimics of (APy) $6[H2W12O40]$. Answer time, repeatability, and shelf life were 10 seconds, 4%, and 60 days, respectively. The LOD was 0.4 M in the presence of covalently bonded SWCNT. A linear plot was achieved in both aspects when the experimental data were viewed as Lineweaver-Burker plots, indicating Michaelis-Menten actions.

Dip-coating n-octyl pyridinium hexafluorophosphate ($[C_8Py][PF_6]$) and 1:12 phosphomolybdic acid (PMO_{12}) on glassy carbon electrodes modified using multiwall carbon nanotubes (GCE/MWCNTs) resulted in the formation of n-octyl pyridinium hexafluorophosphate ($[C_8Py][PF_6]$), as reported by Haghighi et al. [93] who generated a robust and stable layer. The cyclic voltammograms of the GCE/MWCNTs/$[C_8Py]$ $[PF_6]$- PMO_{12} system exhibited three well-defined pairs of redox peaks attributable to the PMO_{12} system. The reduction of H_2O_2 and iodate was electrocatalyst with high efficiency by the GCE/MWCNTs/$[C_8Py][PF_6]$-PMO_{12}. With a correlation coefficient of 0.9999, the calibration plot for H_2O_2 determination is linear between 2×10^{-5} and 8×10^{-3} M. The LODs for H_2O_2 (signal to noise ratio = 3) and sensor sensitivity are 12 M and 73 A mM^{-1} cm^{-2}, respectively. Amperometric tests were also performed to determine IO_3^-. The IO_3^- detector calibration plot was linear between 2×10^{-3} M and 2×10^{-5} M, with LODs and sensibility of 190 A mM^{-1} cm^{-2} and 15 M, respectively.

4.2. POM-conductive polymer composites

The redox-active substrate binding sites of the molecularly scattered POMs signal the presence of substrates, whereas the CP translates the signal into electrical information for greater (quantitative) detection, making POM/CPs ideal composites for substrate sensing [80, 81, 94]. A composite film of Dawson anions trapped in electropolymerized PPy has recently been claimed by Anwar et al. [95]. With a 0.3 mM LOD, the compounds were employed as hydrogen peroxide amperometric sensors. In a pH range of 2–7, voltammetric analyses of redox processes were connected to all components, indicating highly stable redox reactions. Only transition-metal-functionalized Dawson anions (M = Fe^{3+}, Cu^{2+}, Co^{2+}) ($[P_2W_{17}O_{61}M]n^-$) were used to detect H_2O_2. Fe^{3+} and Cu^{2+} substituted in POM-doped polypyrrole films had LODs of 0.6 and 0.3 µM in order, with a linear region ranging from 0.1 - 2 mM H_2O_2. H_2O_2 was detected using only transition-metal functionalized Dawson anions (M =Fe^{3+}, Cu^{2+}, Co^{2+}) ($[P_2W_{17}O_{61}M]n^-$) . Cu^{2+} and Fe^{3+} substituted POM-doped polypyrrole films having a linear area extending from 0.1 to 2 mM for H_2O_2 had LODs of 0.3 and 0.6 µM, correspondingly.

Ammam et al. [96] reported using the composition of POM/CP for gas sensing, demonstrating that the nanostructured composition of POM/PPy can be utilized for the detection of NOx. The Dawson anion P_2Mo_{18} was used as an oxidant to polymerize pyrrole in situ. The resultant semiconducting composite had high selectivity for gaseous NOx detection and a wide NO_x-concentration-dependent linear response. They used a hybrid material made of polypyrrole and $K_6P_2Mo_{18}O_{62}.nH_2O$ to create sensitive and selective NO_x sensors with broad linearity (up to 5500 ppm NO_x).

Ayranci et al. [97] devised a new composite film-based amperometric glucose sensor, made via electrochemical polymerization of carbazole derivatives with free amino groups being of the Keggin kind of POM anion, ($nBu_4N)_3[PW_9O_{34}(tBuSiOH)_3]$. POM was entrapped in the produced PAAC polymer film during the electropolymerization process of 3-amino-9-ethyl carbazole (AAC) on the graphite electrode. Negatively charged POM structures were used to create a metal/organic conducting polymeric composite and a positively charged PAAC-based conducting polymer. The amperometric response of the POM/PAAC-GOx modified electrode was investigated by varying concentrations of glucose

at a potential of -0.7 V (Ag/AgCl). Among the composition structures synthesized at different ratios, the composite structure of POM/PAAC, owing to the best sensor response, had the lowest oxidation potential. The POM/PAAC sensor device had a sensitivity of 66.66μA mM^{-1}cm^{-2} for actual glucose detections, with a LOD of 0.099 mm and a linear LOD of 0.1-10 mm. Because of the multiple redox reactions, rapid electron transfer, and high reactivity of POMs, the composition of POM/PACC possesses a desirable structure. This composite, in particular, showed a rapid response time with high electrocatalytic activity for amperometric glucose detection, reproducibility, and good sensitivity, as well as simple preparation as prepared and acceptable recovery (Fig. 4).

By using the cyclic voltammetry (CV) approach, Babakhanian et al. [82] electrochemically produced (-POM) (K7PMO2W9O39.H2O) and AuNPs doped into electropolymerized polypyrrole (PPy) film. The PPy–POM–AuNPs modified gold (Au) electrode was used to determine folic acid (FA) using square-wave voltammetry (SWV). With an electron transfer rate constant (ks) of 1.15   10^{19} s^{-1} at 0.3 V (vs. SCE), the improved electrode demonstrated better electrocatalytic capability in the reduction of FA. Common coexisting chemicals did not affect the changed electrode response to FA. The LOD and RSD measurements of the proposed method achieved 0.12 nM and 5.3%, respectively, for eight repeated measurements. During the experiments, the modified electrode demonstrated high-level stability and repeatable behavior, making it ideal for analytical applications (Fig. 5).

The synthesis of polypyrrole-polyoxometalate hybrid polymer films and their performance for resistive-type humidity sensors were reported by Miao et al. [98]. Co-electrodeposition of free pyrrole units with metal oxide groups resulted in hybrid polymer films of various thicknesses. A 59 nm-hick sample with a sensing range of 11-98% relative humidity revealed a sensing answer of 1.9 s and a healing process of 1.1 s at 98% humidity levels and a sensing range of 11-98% humidity. The physicochemical properties of the oxidation doping component and the proton acid doping component might be explained by considerable sensitivity in the polypyrrole chain. Even after two months, the nanocomposite-based humidity sensor was repeatable, with recovery times and good response. It was discovered that as the humidity level rose, the sensor conductance rose as well.

4.3. POM-metal composites

Because of their proton and electron storage and/or transfer abilities, POMs can emerge as effective acceptors or donors of numerous electrons in reduced forms without undergoing any structural changes. Reduced POMs have been shown to act with both capping and reductants for POMs, and noble-metal NPs have also been identified as green reduction/oxidation and environmentally friendly agents [64, 83, 99].

Wang et al. [100] synthesized Pd/POMs/NHCSs tri-component nanohybrids with the catalytic rate constant (kcat) of 2.34103 M^{-1}s^{-1} and electrocatalytic activity for oxidized acetaminophen (AP) with a diffusion coefficient (D) of 6.1810^{-5} cm^{2}s^{-1} due to the synergistic actions of NPs, Pd, and NHCSs. They evaluated the usage of POMs/Pd/NHCSs as an effect on determining the template of AP for electrochemical detection, which demonstrated exceptional analytical performance, including a linear region of 0.02-0.63 μM with a sensitivity of 508.46 AmM^{-1}, a linear range of 0.63 M to 0.083 mM with a low LOD of 3 nM, and sensitivity of 154.27 μAmM^{-1}.

They produced a Pd/POMs/NHCSs-GCE-based sensitive electrochemical sensor for AP that had a broad linear range, superior sensitivity, low LOD, and high stability. Karimi-Maleh et al. [101] developed an N-hydroxysuccinimide sensor using a carbon paste electrode (CPE) amplified with a 1-hexyl-3-methylimidazolium chloride (HMICl) and tri-component nanohybrid composite (Platinum nanoparticle/Polyoxometalate/two-dimensional hexagonal boron nitride nanosheets) (PtNPs/

POM/2D-hBN) as conductive mediators. HMIClPtNPs/POM/2D-hBN/POMBNS/CPE led to a remarkable reduction (110 mV) in oxidation overvoltage and a considerable increase (2.4 times) in the N-hydroxysuccinimide current. Moreover, the HMICl- PtNPs/POM/2DhBN/POMBNS/CPE showed high linearity from 0.1 to 300 μM and a LOD of 60 nM for N-hydroxysuccinimide determination. The ability to promote electron exchange between HMICl-PtNPs/POM/2D-hBN/POMBNS/CPE and N-hydroxysuccinimide demonstrated a novel analytical trend to fabricate a water pollutant sensor. In comparison to other electrodes, the PtNPs/POM/2D-hBN presented excellent characteristics such as great specific surface area and high electrical conductivity, as well as the role of HMICl as a conductive binder, helping to modify the oxidation signal of N-hydroxysuccinimide at the surface of HMICl-PtNPs/POM/2D-hBN/POMBNS/CPE.

Zhang et al. [102] developed a remarkably sensitive non-enzymatic electrochemical sensor based on an inorganic-organic nanocomposite film made up of chitosan-palladium (Cs-Pd) that was used to measure ascorbic acid (AA) and H$_7$P$_2$Mo$_{17}$V$_1$O$_{62}$ (P$_2$Mo$_{17}$V), Ru(bpy)$_3$Cl$_2$·6H$_2$O (Ru(bpy)$_3$). Because of the composition of three active components in the latest film, the non-enzymatic sensor has some benefits, including excellent sensitivity, simple production and operation, and good reproducibility, which overcome the disadvantages of enzyme-based sensors such as fast inactivation and limited immobilization. The sensor has excellent sensing performance for ascorbic acid detection with a low LOD of 0.1 μM (S/N = 3), a fast response time of 2 seconds, and a wide linear range of 0.125 – 118 μM. The sensor was also used to detect AA in juice with success. Zhou et al. [65] produced a new composite film based on Dawson-type phosphovanadotungstate K$_8$P$_2$W$_{16}$V$_2$O$_{62}$·18H$_2$O (P$_2$W$_{16}$V$_2$) decorated with Au–Pd alloy nanoparticles (Au–Pd) on quartz, ITO and silicon by the layer-by-layer self-assembly technique. The mixture film can be used to identify ascorbic acid and dopamine at biological pH in a simultaneous and sensitive determination (pH 7.0). Linear curves were achieved in the ranges of 1.2 × 10^{-6}-1.61 × 10^{-3} M and 2.1 × 10^{-6}-2.06 × 10^{-3} M for ascorbic acid and dopamine in order, by DPV procedures. Dopamine and ascorbic acid had low LODs of 8.3 × 10^{-7} M and 4.3 × 10^{-7}, respectively. Ascorbic acid and dopamine determinations in real samples were performed successfully using the composite film. The proposed electrochemical sensor has high selectivity and sensitivity, making it a simple method for determining ascorbic acid and dopamine simultaneously in practical applications (Fig. 6).

5. Conclusions and future insight

This literature review provided an overview of the promising performance of POMs and POM-based composites as well as their structures and properties. The structure of these materials varies from Keggin and Dawson to a variety of other structures such as wheels, sandwiches, bananas, and other forms. POMs-based composites have attracted much attention because of their multitudinous architectures and excellent redox activities as well as convenient proton and electron transport capacities, which are one of the candidates for functional components in a variety of functions, according to the findings. This review specifically highlighted the use of POM-based composites as sensors. A more detailed focus has been made on the combination of POMs and nanocarbon structures owing to the extensive availability and cost-effectiveness of POM/nanocarbon composites. A combination of nanostructured carbons and POMs, combining the excellent electronic properties of nanocarbon with the outstanding chemical reactivity of POMs, has led to its application in amperometric sensors mainly due to their alterable multi-electron redox behavior. The future growth of POM/nanocarbon compositions is not limited. There are joint projects that combine polyoxometalate chemists, device fabrication experts, and experience of nanocarbon expertise fo-

cusing on real-life technology that can produce self-assembled POM and nanocarbon components. As it can be seen, investigating novel materials with higher proton and electron conductivity, activity, and stability is always essential in promising technologies and is found to capture the way for future development of POM science, for which POMs are one of those promising materials.

Acknowledgments

Conflict of interest

The authors declare that there is no conflict of interest.

REFERENCES

[1] M. Ammam, Polyoxometalates: Formation, structures, principal properties, Main Deposition Methods and Application in Sensing, Journal of Materials Chemistry A 1(21) (2013) 6291-6312.

[2] X. An, Q. Tang, H. Lan, H. Liu, J. Qu, Polyoxometalates/TiO_2 Fenton-like photocatalysts with rearranged oxygen vacancies for enhanced synergetic degradation, Applied Catalysis B: Environmental 244 (2019) 407-413.

[3] S. Li, G. Li, P. Ji, J. Zhang, S. Liu, J. Zhang, X. Chen, A Giant Mo/Ta/W Ternary Mixed-Addenda Polyoxometalate with Efficient Photocatalytic Activity for Primary Amine Coupling, ACS Applied Materials & Interfaces 11(46) (2019) 43287-43293.

[4] L. Bazli, M.H. Bagherian, M. Karrabi, F. Abbassi-Sourki, H. Azizi, Effect of starch ratio and compatibilization on the viscoelastic behavior of POE/starch blends, Journal of Applied Polymer Science 137(29) (2020) 48877.

[5] A. Misra, K. Kozma, C. Streb, M. Nyman, Beyond Charge Balance: Counter-Cations in Polyoxometalate Chemistry, Angewandte Chemie International Edition 59(2) (2020) 596-612.

[6] N.I. Gumerova, A. Rompel, Polyoxometalates in solution: speciation under spotlight, Chemical Society Reviews 49(21) (2020) 7568-7601.

[7] Z.-F. Chen, Y.-L. Yang, C. Zhang, S.-Q. Liu, J. Yan, Manufacture of non-aqueous redox flow batteries using sulfate-templated Dawson-type polyoxometalate with improved performances, Journal of Energy Storage 35 (2021) 102281.

[8] Q. Chen, C. Shen, L. He, Recent advances of polyoxometalate-catalyzed selective oxidation based on structural classification, Acta Crystallographica Section C: Structural Chemistry 74(11) (2018) 1182-1201.

[9] J. Xu, Z. Zhang, K. Yang, W. He, X. Yang, X. Du, L. Meng, P. Zhao, Z. Wang, Construction of new transport channels by blending POM-based inorganic-organic complex into sulfonated poly(ether ketone sulfone) for proton exchange membrane fuel cells, Journal of Membrane Science 596 (2020) 117711.

[10] D. Wang, L. Liu, J. Jiang, L. Chen, J. Zhao, Polyoxometalate-based composite materials in electrochemistry: state-of-the-art progress and future outlook, Nanoscale 12(10) (2020) 5705-5718.

[11] C. Boskovic, Rare earth polyoxometalates, Accounts of Chemical Research 50(9) (2017) 2205-2214.

[12] A. Al-Yasari, H. El Moll, R. Purdy, K.B. Vincent, P. Spence, J.-P. Malval, J. Fielden, Optical, third order non-linear optical and electrochemical properties of dipolar, centrosymmetric and C_{2v} organoimido polyoxometalate derivatives, Physical Chemistry Chemical Physics 23(20) (2021) 11807-11817.

[13] M. Guzel, Y. Torlak, E. Karatas, M. Ak, Optical and electrical properties of monolacunary Keggin-type polyoxometalate/star-shaped polycarbazole nanocomposite film, Journal of Electrochemical Society 166(8) (2019) H313.

[14] J. Lei, J.J. Yang, T. Liu, R.M. Yuan, D.R. Deng, M.S. Zheng, J.J. Chen, L. Cronin, Q.F. Dong, Tuning Redox Active Polyoxometalates for Efficient Electron-Coupled Proton-Buffer-Mediated Water Splitting, Chemistry (Weinheim an der Bergstrasse, Germany) 25(49) (2019) 11432.

[15] X. Wei, K. Ma, Y. Cheng, L. Sun, D. Chen, X. Zhao, H. Lu, B. Song, K. Yang, P. Jia, Adhesive, Conductive, Self-Healing, and Antibacterial Hydrogel Based on Chitosan–Polyoxometalate Complexes for Wearable Strain Sensor, ACS Applied Polymer Materials 2(7) (2020) 2541-2549.

[16] Y. Xia, P. Wu, Y. Wei, Y. Wang, H. Guo, Synthesis, Crystal Structure, and Optical Properties of a Polyoxometalate-Based Inorganic−Organic Hybrid Solid, (n-Bu4N)2[Mo6O17(≡NAr)2] (Ar = o-CH3OC6H4), Crystal Growth & Design 6(1) (2006) 253-257.

[17] P. Ma, F. Hu, J. Wang, J. Niu, Carboxylate covalently modified polyoxometalates: From synthesis, structural diversity to applications, Coordination Chemistry Reviews 378 (2019) 281-309.

[18] S. Derakhshanrad, M. Mirzaei, C. Streb, A. Amiri, C. Ritchie, Polyoxometalate-based frameworks as adsorbents for drug of abuse extraction from hair samples, Inorganic Chemistry 60(3) (2021) 1472-1479.

[19] Y.-L. Zou, H.-Y. Li, W. Zhou, X.-G. Cui, G.-H. Zou, G.-Z. Shen, Introduction of the antibacterial drugs norfloxacin and Ciprofloxacin into a polyoxometalate structure: Synthesis, characterization, and antibacterial activity, Journal of Molecular Structure 1205 (2020) 127584.

[20] T.R. Bastami, A. Ahmadpour, Preparation of magnetic photocatalyst nanohybrid decorated by polyoxometalate for the degradation of a pharmaceutical pollutant under solar light, Environmental Science and Pollution Research 23(9) (2016) 8849-8860.

[21] H. Wu, M. Zhi, H. Chen, V. Singh, P. Ma, J. Wang, J. Niu, Well-tuned white-light-emitting behaviours in multicenter-Ln polyoxometalate derivatives: A photoluminescence property and energy transfer pathway study, Spectrochimica Acta Part A: Molecular and Biomolecular Spectroscopy 223 (2019) 117294.

[22] S.A. Alshehri, A. Al-Yasari, F. Marken, J. Fielden, Covalently Linked Polyoxometalate–Polypyrrole Hybrids: Electropolymer Materials with Dual-Mode Enhanced Capacitive Energy Storage, Macromolecules 53(24)(2020) 11120-11129.

[23] M.R. Horn, A. Singh, S. Alomari, S. Goberna-Ferrón, R. Benages-Vilau, N. Chodankar, N. Motta, K.K. Ostrikov, J. MacLeod, P. Sonar, Polyoxometalates (POMs): from electroactive clusters to energy materials, Energy & Environmental Science 14(4) (2021) 1652-1700.

[24] X. Xin, N. Hu, Y. Ma, Y. Wang, L. Hou, H. Zhang, Z. Han, Polyoxometalate-based crystalline materials as a highly sensitive electrochemical sensor for detecting trace Cr (VI), Dalton Transactions 49(14) (2020) 4570-4577.

[25] C. Zhou, S. Li, W. Zhu, H. Pang, H. Ma, A sensor of a polyoxometalate and Au–Pd alloy for simultaneously detection of dopamine and ascorbic acid, Electrochimica Acta 113 (2013) 454-463.

[26] C. Sabarinathan, M. Karthikeyan, R. Murugappan, S.P. Anthony, B. Shankar, K. Parthasarathy, T. Arumuganathan, Polyoxometalate based ionic crystal: dual applications in selective colorimetric sensor for hydrated $ZnCl_2$ and antimicrobial activity, New Journal of Chemistry 45(12) (2021) 5576-5588.

[27] J. Zhong, J. Pérez-Ramírez, N. Yan, Biomass valorisation over polyoxometalate-based catalysts, Green Chemistry 23(1) (2021) 18-36.

[28] M.A. Rezvani, M. Shaterian, M. Aghmasheh, Catalytic oxidative desulphurization of gasoline using amphiphilic polyoxometalate@ polymer nanocomposite as an efficient, reusable, and green organic–inorganic hybrid catalyst, Environmental technology 41(10) (2020) 1219-1231.

[29] N. Mizuno, K. Kamata, K. Yamaguchi, Green oxidation reactions by polyoxometalate-based catalysts: from molecular to solid catalysts, Topics in Catalysis 53(13-14) (2010) 876-893.

[30] C.G. Lin, J. Hu, Y.F. Song, Polyoxometalate-Functionalized Nanocarbon Materials for Energy Conversion, Energy Storage, and Sensor Systems, Advances in Inorganic Chemistry, Academic Press, Cambridge, MA, USA, 2017, pp. 181-212.

[31] Y. Ji, L. Huang, J. Hu, C. Streb, Y.-F. Song, Polyoxometalate-functionalized nanocarbon materials for energy conversion, energy storage and sensor systems, Energy & Environmental Science 8(3) (2015) 776-789.

[32] Q. Li, A. Tian, C. Chen, T. Jiao, T. Wang, S. Zhu, J. Sha, Anderson polyoxometalates with intrinsic oxidase-mimic activity for "turn on" fluorescence sensing of dopamine, Analytical and Bioanalytical Chemistry 413(16) (2021) 4255-4265.

[33] J. Marignac, Recherches chimiques et cristallographiques sur les fluozirconates, Annales de chimie et de physique 60 (1860) 257-307.

[34] J. Du, Z.-L. Lang, Y.-Y. Ma, H.-Q. Tan, B.-L. Liu, Y.-H. Wang, Z.-H. Kang, Y.-G. Li, Polyoxometalate-based electron transfer modulation for efficient electrocatalytic carbon dioxide reduction, Chemical Science 11(11) (2020) 3007-3015.

[35] B. Huang, D. Ke, Z. Xiong, Y. Wang, K. Hu, P. Jiang, M. Liang, Z. Xiao, P. Wu, Covalent hybrid materials between polyoxometalates and organic molecules for enhanced electrochemical properties, Journal of Materials Science 55(13) (2020) 5554-5570.

[36] M.S. Nunes, P. Neves, A.C. Gomes, L. Cunha-Silva, A.D. Lopes, A.A. Valente, M. Pillinger, I.S. Gonçalves, A silicododecamolybdate/pyridinium-tetrazole hybrid molecular salt as a catalyst for the epoxidation of bio-derived olefins, Inorganica Chimica Acta 516 (2021) 120129.

[37] P. Liu, Y. Liang, X. Lin, C. Wang, G. Yang, A General Strategy To Fabricate Simple Polyoxometalate Nanostructures: Electrochemistry-Assisted Laser Ablation in Liquid, ACS Nano 5(6) (2011) 4748-4755.

[38] P. He, W. Chen, J. Li, H. Zhang, Y. Li, E. Wang, Keggin and Dawson polyoxometalates as electrodes for flexible and transparent piezoelectric nanogenerators to efficiently utilize mechanical energy in the environment, Science Bulletin 65(1) (2020) 35-44.

[39] L. Pauling, The molecular structure of the tungstosilicates and related com-

pounds, Journal of the American Chemical Society 51(10) (1929) 2868-2880.

[40] J.F. Keggin, Structure of the molecule of 12-phosphotungstic acid, Nature 131(3321) (1933) 908-909.

[41] J. Macht, M.J. Janik, M. Neurock, E. Iglesia, Catalytic consequences of composition in polyoxometalate clusters with Keggin structure, Angewandte Chemie 119(41) (2007) 8010-8014.

[42] A. Kondinski, T.N. Parac-Vogt, Keggin structure, quō vādis?, Frontiers in chemistry 6 (2018) 346.

[43] W.A. Neiwert, J.J. Cowan, K.I. Hardcastle, C.L. Hill, I.A. Weinstock, Stability and Structure in α-and β-Keggin Heteropolytungstates,$[X^{n+}W_{12}O_{40}]^{(8-n)-}$, X= p-Block Cation, Inorganic chemistry 41(26) (2002) 6950-6952.

[44] J.M. Clemente-Juan, E. Coronado, A. Forment-Aliaga, J.R. Galán-Mascarós, C. Giménez-Saiz, C.J. Gómez-García, A new heptanuclear cobalt (II) cluster encapsulated in a novel heteropolyoxometalate topology: synthesis, structure, and magnetic properties of $[Co_7 (H_2O)_2(OH)_2P_2W_{25}O_{94}]16-$, Inorganic chemistry 43(8) (2004) 2689-2694.

[45] M. Ammam, B. Keita, L. Nadjo, I.M. Mbomekalle, M.D. Ritorto, T.M. Anderson, W.A. Neiwert, C.L. Hill, J. Fransaer, Cyclic Voltammetry Study of the Mn-Substituted Polyoxoanions $[Mn^{II4}(H_2O)_2 (H_4AsW_{15}O_{56})_2]^{18-}$ and $[((Mn^{II}OH_2) Mn^{II2}PW_9O_{34})_2(PW_6O_{26})]^{17-}$: Electrodeposition of Manganese Oxides Electrocatalysts for Dioxygen Reduction, Electroanalysis 23(6) (2011) 1427-1434.

[46] P. Souchay, Contribution a letude des phenomenes de condensation en chimie minerale. 1. Critique des mesures de diffusion et dialyse, Bulletin De La Societe Chimique De France 14(9-10) (1947) 914-924.

[47] H. Wu, M. Zhi, C. Chen, Y. Zhu, P. Ma, J. Wang, J. Niu, Synthesis, characterization, and photoluminescence properties of three two-dimensional lanthanide-containing Dawson-type polyoxometalates, Dalton Transactions 48(36) (2019) 13850-13857.

[48] A. Iqbal, H.M. Asif, Y. Zhou, L. Zhang, T. Wang, F. Khurum Shehzad, X. Ren, From simplicity to complexity in grafting Dawson-type polyoxometalates on porphyrin, leading to the formation of new organic–inorganic hybrids for the investigation of third-order optical nonlinearities, Inorganic Chemistry 58(13) (2019) 8763-8774.

[49] T.J. Weakley, H.T. Evans, J.S. Showell, G.F. Tourné, C.M. Tourné, 18-Tungstotetracobalto (II) diphosphate and related anions: a novel structural class of heteropolyanions, Journal of the Chemical Society, Chemical Communications (4) (1973) 139-140.

[50] I.M. Mbomekalle, B. Keita, M. Nierlich, U. Kortz, P. Berthet, L. Nadjo, Structure, Magnetism, and Electrochemistry of the Multinickel Polyoxoanions $[Ni_6As_3W_{24}O_{94} (H_2O)_2]^{17-}$,$[Ni_3Na(H_2O)_2(AsW_9O_{34})_2]^{11-}$, and $[Ni_4Mn_2P_3W_{24}O_{94}(H_2O)_2]^{17-}$, Inorganic Chemistry 42(17) (2003) 5143-5152.

[51] M.D. Ritorto, T.M. Anderson, W.A. Neiwert, C.L. Hill, Decomposition of A-Type Sandwiches. Synthesis and Characterization of New Polyoxometalates Incorporating Multiple d-Electron-Centered Units, Inorganic Chemistry 43(1) (2004) 44-49.

[52] S.T. Zheng, J. Zhang, G.Y. Yang, Designed synthesis of POM–organic frameworks from $\{Ni_6PW_9\}$ building blocks under hydrothermal conditions, Angewandte Chemie 120(21) (2008) 3973-3977.

[53] Y. Zhang, L. Zhang, Z. Hao, F. Luo, Controlling the synthesis of novel chiral polyoxometalate-based compounds and racemic compounds from the same system, Dalton Transactions 39(30) (2010) 7012-7016.

[54] S. Zhang, Y. Lu, X.-W. Sun, Z. Li, T.-Y. Dang, Z. Zhang, H.-R. Tian, S.-X. Liu, Purely inorganic frameworks based on polyoxometalate clusters with abundant phosphate groups: single-crystal to single-crystal structural transformation and remarkable proton conduction, Chemical Communications 56(3) (2020) 391-394.

[55] I.V. Kozhevnikov, Catalysis by Heteropoly Acids and Multicomponent Polyoxometalates in Liquid-Phase Reactions, Chemical Reviews 98(1) (1998) 171-198.

[56] N. Kashyap, S. Das, R. Borah, Chapter-9 A Brief Insight into the Polyoxometalate Based Organic-Inorganic Hybrid Systems and their Catalytic uses in Oxidation and Acid Catalyzed Organic Reactions, Chemical Sciences 1 (2020) 167.

[57] I.M. Mbomekalle, B. Keita, L. Nadjo, K.I. Hardcastle, C.L. Hill, T.M. Anderson, Semi-vacant Wells–Dawson anions. Synthesis of tri-tungsten-vacant derivatives and crystallographic studies of $[\alpha\beta\beta\alpha$-$(Cu^{II}OH_2)_2 (Cu^{II})_2(AsW_{15}(OH_2)_3(OH) O_{52})_2]^{12-}$, Dalton Transactions (24) (2004) 4094-4095.

[58] J. Lehmann, A. Gaita-Arino, E. Coronado, D. Loss, Spin qubits with electrically gated polyoxometalate molecules, Nature Nanotechnology 2(5) (2007) 312-317.

[59] B.S. Bassil, U. Kortz, 2.5 Polyoxometalates, Rare Earth Chemistry (2020) 171.

[60] W. Xu, J.-F. Cao, Y.-N. Lin, Y. Shu, J.-H. Wang, Functionalized polyoxometalate microspheres ensure selective adsorption of phosphoproteins and glycoproteins, Chemical Communications 57(27) (2021) 3367-3370.

[61] W. Salomon, A. Dolbecq, C. Roch-Marchal, G. Paille, R. Dessapt, P. Mialane, H. Serier-Brault, A Multifunctional Dual-Luminescent Polyoxometalate@ Metal-Organic Framework EuW10@UiO-67 Composite as Chemical Probe and Temperature Sensor, Frontiers in Chemistry 6 (2018) 410815.

[62] A. Kaczmarek, J. Liu, B. Laforce, L. Vincze, K. Van Hecke, R. Van Deun, Cryogenic luminescent thermometers based on multinuclear Eu^{3+}/Tb^{3+} mixed lanthanide polyoxometalates, Dalton Transactions 46(18) (2017) 5781-5785.

[63] D. Çimen, A. Denizli, Development of rapid, sensitive, and effective plasmonic nanosensor for the detection of vitamins in infact formula and milk samples, Photonic Sensors 10(2020) 1-17.

[64] A. Babakhanian, S. Kaki, M. Ahmadi, H. Ehzari, A. Pashabadi, Development of α-polyoxometalate–polypyrrole–Au nanoparticles modified sensor applied for detection of folic acid, Biosensors and Bioelectronics 60 (2014) 185-190.

[65] L. Wang, T. Meng, J. Sun, S. Wu, M. Zhang, H. Wang, Y. Zhang, Development of Pd/Polyoxometalate/nitrogen-doping hollow carbon spheres tricomponent nanohybrids: a selective electrochemical sensor for acetaminophen, Analytica Chimica Acta 1047 (2019) 28-35.

[66] N. Li, J. Liu, B.X. Dong, Y.Q. Lan, Polyoxometalate-Based Compounds for Photo-and Electrocatalytic Applications, Angewandte Chemie 132(47) (2020) 20963-20977.

[67] L. Zhang, S. Li, K.P. O'Halloran, Z. Zhang, H. Ma, X. Wang, L. Tan, H. Pang, A highly sensitive non-enzymatic ascorbic acid electrochemical sensor based on polyoxometalate/Tris (2, 2´-bipyridine) ruthenium (II)/chitosan-palladium inorganic-organic self-assembled film, Colloids and Surfaces A: Physicochemical and Engineering Aspects 614 (2021) 126184.

[68] Z. Bai, C. Zhou, H. Xu, G. Wang, H. Pang, H. Ma, Polyoxometalates-doped Au nanoparticles and reduced graphene oxide: a new material for the detection of uric acid in urine, Sensors and Actuators B: Chemical 243 (2017) 361-371.

[69] J. Zhang, Y. Huang, G. Li, Y. Wei, Recent advances in alkoxylation chemistry of polyoxometalates: From synthetic strategies, structural overviews to functional applications, Coordination Chemistry Reviews 378 (2019) 395-414.

[70] H. Shi, N. Li, Z. Sun, T. Wang, L. Xu, Interface modification of titanium dioxide nanoparticles by titanium-substituted polyoxometalate doping for improvement of photoconductivity and gas sensing applications, Journal of Physics and Chemistry of Solids 120 (2018) 57-63.

[71] Y. Shen, J. Peng, H. Zhang, C. Meng, F. Zhang, Preparation and application of L-cysteine-doped Keggin polyoxometalate microtubes, Journal of Solid State Chemistry 185 (2012) 225-228.

[72] H. Medetalibeyoğlu, M. Beytur, S. Manap, C. Karaman, F. Kardaş, O. Akyıldırım, G. Kotan, H. Yüksek, N. Atar, M.L. Yola, Molecular Imprinted Sensor Including Au Nanoparticles/Polyoxometalate/Two-Dimensional Hexagonal Boron Nitride Nanocomposite for Diazinon Recognition, ECS Journal of Solid State Science and Technology 9(10) (2020) 101006.

[73] H. Lin, K.S. Suslick, A colorimetric sensor array for detection of triacetone triperoxide vapor, Journal of the American Chemical Society 132(44) (2010) 15519-15521.

[74] A. Üzer, S. Durmazel, E. Erçağ, R. Apak, Determination of hydrogen peroxide and triacetone triperoxide (TATP) with a silver nanoparticles—based turn-on colorimetric sensor, Sensors and Actuators B: Chemical 247 (2017) 98-107.

[75] X. Lü, P. Hao, G. Xie, J. Duan, L. Gao, B. Liu, A Sensor Array Realized by a Single Flexible TiO2/POMs Film to Contactless Detection of Triacetone Triperoxide, Sensors 19(4) (2019) 915.

[76] J. Qian, K. Wang, Y. Jin, X. Yang, L. Jiang, Y. Yan, X. Dong, H. Li, B. Qiu, Polyoxometalate@ magnetic graphene as versatile immobilization matrix of Ru $(bpy)_3^{2+}$ for sensitive magneto-controlled electrochemiluminescence sensor and its application in biosensing, Biosensors and Bioelectronics 57 (2014) 149-156.

[77] Ö.A. Yokuş, F. Kardaş, O. Akyıldırım, T. Eren, N. Atar, M.L. Yola, Sensitive voltammetric sensor based on polyoxometalate/reduced graphene oxide nanomaterial: application to the simultaneous determination of l-tyrosine and l-tryptophan, Sensors and Actuators B: Chemical 233 (2016) 47-54.

[78] M.L. Yola, N. Atar, T. Eren, H. Karimi-Maleh, S. Wang, Sensitive and selective determination of aqueous triclosan based on gold nanoparticles on polyoxometalate/reduced graphene oxide nanohybrid, Rsc Advances 5(81) (2015) 65953-65962.

[79] Z. Li, J. Chen, D. Pan, W. Tao, L. Nie, S. Yao, A sensitive amperometric bromate sensor based on multi-walled carbon nanotubes/phosphomolybdic acid composite film, Electrochimica Acta 51(20) (2006) 4255-4261.

[80] B. Ertan, T. Eren, İ. Ermiş, H. Saral, N. Atar, M.L. Yola, Sensitive analysis of simazine based on platinum nanoparticles on polyoxometalate/multi-walled carbon nanotubes, Journal of Colloid and Interface Science 470 (2016) 14-21.

[81] B. Haghighi, H. Hamidi, L. Gorton, Formation of a robust and stable film

comprising ionic liquid and polyoxometalate on glassy carbon electrode modified with multiwalled carbon nanotubes: Toward sensitive and fast detection of hydrogen peroxide and iodate, Electrochimica Acta 55(16) (2010) 4750-4757.

[82] N. Anwar, M. Vagin, F. Laffir, G. Armstrong, C. Dickinson, T. McCormac, Transition metal ion-substituted polyoxometalates entrapped in polypyrrole as an electrochemical sensor for hydrogen peroxide, Analyst 137(3) (2012) 624-630.

[83] R. Ayranci, Y. Torlak, T. Soganci, M. Ak, Trilacunary Keggin type polyoxometalate-conducting polymer composites for amperometric glucose detection, Journal of The Electrochemical Society 165(13) (2018) B638.

[84] H. Karimi-Maleh, F. Karimi, S. Malekmohammadi, N. Zakariae, R. Esmaeili, S. Rostamnia, M.L. Yola, N. Atar, S. Movaghgharnezhad, S. Rajendran, An amplified voltammetric sensor based on platinum nanoparticle/polyoxometalate/two-dimensional hexagonal boron nitride nanosheets composite and ionic liquid for determination of N-hydroxysuccinimide in water samples, Journal of Molecular Liquids 310 (2020) 113185.

[85] A. Proust, R. Villanneau, Functionalization of Polyoxometalates : Achievements and Perspectives, in: M.T. Pope, A. Müller (Eds.), Polyoxometalate Chemistry From Topology via Self-Assembly to Applications, Springer Netherlands, Dordrecht, 2001, pp. 23-38.

[86] P. Sun, S. Zhang, Z. Xiang, T. Zhao, D. Sun, G. Zhang, M. Chen, K. Guo, X. Xin, Photoluminescent sensing vesicle platform self-assembled by polyoxometalate and ionic-liquid-type imidazolium gemini surfactants for the detection of $Cr3+$ and $MnO4-$ ions, Journal of Colloid and Interface Science 547 (2019) 60-68.

[87] A. González, N. Gálvez, M. Clemente-León, J.M. Dominguez-Vera, Electrochromic polyoxometalate material as a sensor of bacterial activity, Chemical Communications 51(50) (2015) 10119-10122.

[88] D. Pan, J. Chen, W. Tao, L. Nie, S. Yao, Polyoxometalate-modified carbon nanotubes: new catalyst support for methanol electro-oxidation, Langmuir 22(13) (2006) 5872-5876.

[89] B. Iqbal, X. Jia, H. Hu, L. He, W. Chen, Y.-F. Song, Fabrication of redox-active polyoxometalate-based ionic crystals onto single-walled carbon nanotubes as high-performance anode materials for lithium-ion batteries, Inorganic Chemistry Frontiers 7(6) (2020) 1420-1427.

[90] H. Wei, J. Zhang, N. Shi, Y. Liu, B. Zhang, J. Zhang, X. Wan, A recyclable polyoxometalate-based supramolecular chemosensor for efficient detection of carbon dioxide, Chemical Science 6(12) (2015) 7201-7205.

[91] H. Zhang, A. Xie, Y. Shen, L. Qiu, X. Tian, Layer-by-layer inkjet printing of fabricating reduced graphene-polyoxometalate composite film for chemical sensors, Physical Chemistry Chemical Physics 14(37) (2012) 12757-12763.

[92] J. Qu, X. Zou, B. Liu, S. Dong, Assembly of polyoxometalates on carbon nanotubes paste electrode and its catalytic behaviors, Analytica Chimica Acta 599(1) (2007) 51-57.

[93] W. Guo, L. Xu, F. Li, B. Xu, Y. Yang, S. Liu, Z. Sun, Chitosan-assisted fabrication and electrocatalytic activity of the composite film electrode of heteropolytungstate/carbon nanotubes, Electrochimica Acta 55(5) (2010) 1523-1527.

[94] Y. Sahraoui, S. Chaliaa, A. Maaref, A. Haddad, F. Bessueille, N. Jaffrezic-Renault, Synergistic Effect of Polyoxometalate and Single Walled Carbon Nanotubes on Peroxidase-like Mimics and Highly Sensitive Electrochemical Detection of Hydrogen Peroxide, Electroanalysis 32(4) (2020) 683-689.

[95] J. Hu, Y. Ji, W. Chen, C. Streb, Y.-F. Song, "Wiring" redox-active polyoxometalates to carbon nanotubes using a sonication-driven periodic functionalization strategy, Energy & Environmental Science 9(3) (2016) 1095-1101.

[96] AA.D. Stergiou, M.D. Symes, Organic transformations using electro-generated polyoxometalate redox mediators, Catalysis Today 384-386 (2022) 146-155.

[97] M. Yang, S. Rong, X. Wang, H. Ma, H. Pang, L. Tan, Y. Jiang, K. Gao, Preparation and Application of Keggin Polyoxometalate-based 3D Coordination polymer Materials as Supercapacitors and Amperometric Sensors, ChemNanoMat 7(3) (2021) 299-306.

[98] M. Ammam, E.B. Easton, Advanced NO_x gas sensing based on novel hybrid organic–inorganic semiconducting nanomaterial formed between pyrrole and Dawson type polyoxoanion $[P_2Mo_{18}O_{62}]^{6-}$, Journal of Materials Chemistry 21(22) (2011) 7886-7891.

[99] J. Miao, Y. Chen, Y. Li, J. Cheng, Q. Wu, K.W. Ng, X. Cheng, R. Chen, C. Cheng, Z. Tang, Proton conducting polyoxometalate/polypyrrole films and their humidity sensing performance, ACS Applied Nano Materials 1(2) (2018) 564-571.

[100] M. Lechner, R. Güttel, C. Streb, Challenges in polyoxometalate-mediated aerobic oxidation catalysis: catalyst development meets reactor design, Dalton Transactions 45(42) (2016) 16716-16726.

[101] C. Si, P. Ma, Q. Han, J. Jiao, W. Du, J. Wu, M. Li, J. Niu, A Polyoxometalate-Based Inorganic Porous Material with both Proton and Electron Conductivity by Light Actuation: Photocatalysis for Baeyer–Villiger Oxidation and Cr(VI) Reduction, Inorganic Chemistry 60(2) (2021) 682-691.

[102] J. Xu, Z. Zhu, T. Su, W. Liao, C. Deng, D. Hao, Y. Zhao, W. Ren, H. Lü, Green aerobic oxidative desulfurization of diesel by constructing an Fe-Anderson type polyoxometalate and benzene sulfonic acid-based deep eutectic solvent biomimetic cycle, Chinese Journal of Catalysis 41(5) (2020) 868-876.